CHAPTER 3

A green synthesis of palladium nanoparticles by *Sapindus mukorossi* (*S. mukorossi*) seed extracts and its application in efficient room temperature Suzuki-Miyaura cross-coupling reaction.

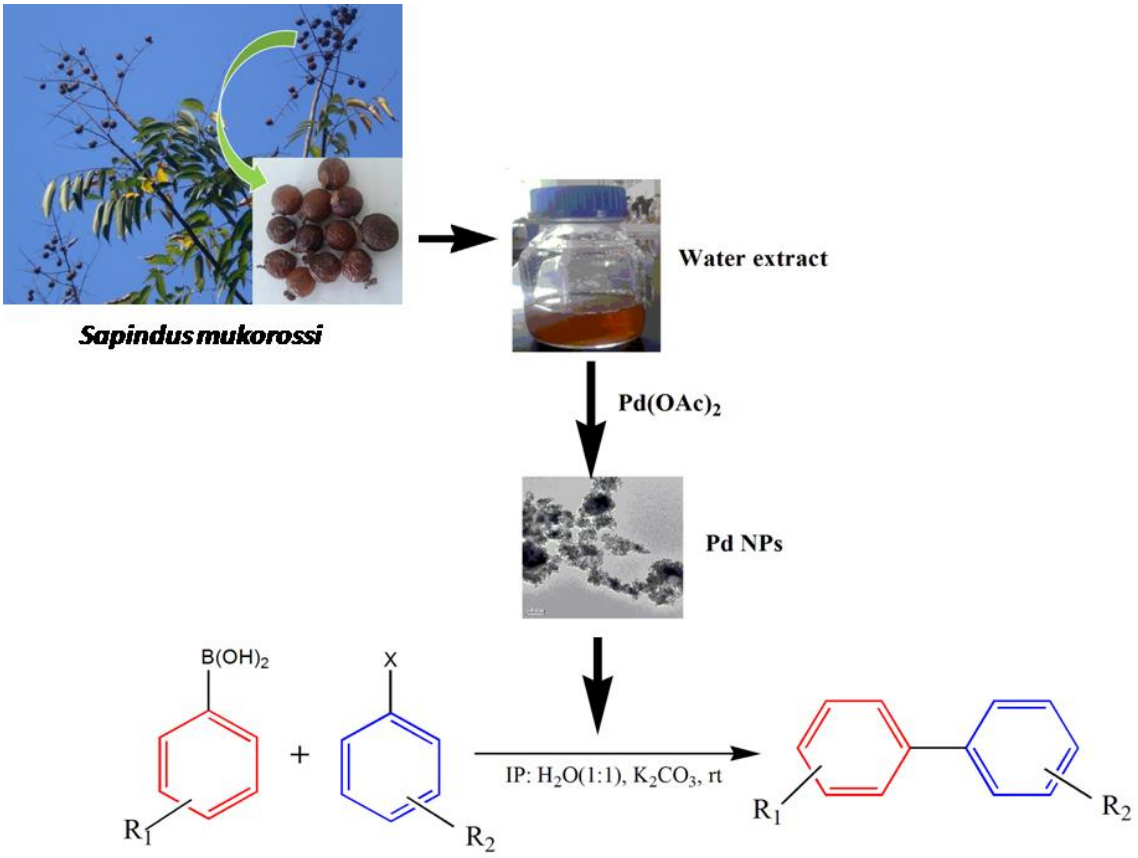

The work described in this chapter has been published in *Applied Organometallic Chemistry*, 2017, e3784

3.1. Introduction

Suzuki-Miyaura cross-coupling reaction is one of the most powerful and widely used methods for the constructing C-C bond, particularly in the formation of biaryls- a structural motif found in many commercially important products [1, 2]. Since, from the initial report [3], the reaction has undergone continous developments so far the catalyst, reaction condition and substrate scopes are concerned. Their ubiquitous use can be attributed to the mild reaction conditions involved and also their compatibility and tolerance to wide range of functional groups. The catalytic system for Suzuki coupling reaction is composed of either Pd(0) or Pd(II) species, and also in some cases suitable phosphine or nitrogen based ligands are added [4]. The Pd catalyzed Suzuki reaction is generally performed under inert atmosphere and also in hazardous organic solvents due to the fact that the catalytic species are sensitive to oxygen and moisture. In addition to this, cost, availability, stability of the Pd species are the additional drawbacks of this reaction. Therefore, nowadays the use of environmently favourable solvents such as water [5], ionic liquids [6], or supercritical carbondioxide [7] are considered to be more favourable alternatives compared to organic solvents which also fullfils the green chemistry perspectives.

Nowadays nano-catalysis is regarded as an emerging area in the field of synthetic organic chemistry. This may be attributed to the peculiar size dependent properties of the NPs [8]. Different physical and chemical methods are generally used for the synthesis of different various shapes and sizes Pd NPs. Generally, in wet chemical methods, reduction of Pd(II) species is done in presence of different types of stabilizing agents [9], capping agents or solid supports, which can control both their size and morphology [10]. Although the synthesized Pd NPs show good catalytic activity yet, these methods are associated with some demerits like requirement of high temperature, ultrasonication etc. thereby making the process tedious and time consuming. In addition, contamination from precursor chemicals, use of toxic solvents and formation of by-products are also associated with these synthetic methods. On the other hand, common physical methods like attrition and pyrolysis requires large energy input. Consequently, there is a continuous demand for the development of alternative methods for the synthesis of NPs which are eco-friendly with minimum loses of chemicals in environmentally friendly solvents.

Biological materials such as plant extracts, microorganisms etc. could be used for the synthesis of NPs [11] as they have the reduction potential required for the reduction of Pd(II) to Pd(0) [12]. The biological methods have a number of advantages over conventional methods such as they are single step process; don't require toxic chemicals or high energy. Generally, the synthesized NPs are thermodynamically not stable which in turn leads to agglomeration and thereby decrease the catalytic activity appreciably. Therefore, different types of stabilizers such as surfactants, organic ligands (viz. sulphur, phosphine and nitrogen based ligands), polymers and dendrimers are used to stabilise the NPs from agglomerization [13]. But, in our case, during the process of synthesizing Pd NPs we didn't use any kind of stabilizers, the functional groups present in the biomolecules of soapnut shell extract itself act as stabilizer and stabilize the resulting Pd NPs formed. Hence, nowadays, these types of cost efficient and environment friendly processes are highly demanding as they can easily be scaled up to industrial goal.

Working in this direction, we already reported a protocol for green synthesis of Pd NPs@PEG from *Colocasia esculanta* leaf extract which could catalyze efficiently Suzuki-Miyaura cross-coupling reaction [14] in the previous chapter. In this chapter, we report a green an efficient method for the generation of Pd NPs by *Sapindus mukorossi* (*S. mukorossi*) seed extract and its successive utilisation in Suzuki-Miyaura cross-coupling reaction at room temperature. The *S. mukorossi* fruit, locally known as 'monisol'or 'ritha' (Fig. 1) is locally available in the north-eastern region of India. The fruit generally appears in the month of July-August and ripens by November-December and can be stored for years after drying. Though the usefulness of the fruit as natural surfactant and medicine sustained from ancient times, yet a few scientific reports have been made only recently that too are not extensive and detailed. Balakrishnan and his co-workers have characterized the saponin content and surfactant property of the dried pericarp of the soapnut fruit [15]. There are reports available in the literature which shows its application in essential oil recovery, in the synthesis of Ag NPs, Au NPs [16] and nanohydroxyapatites. Based on the available reports, we attempted to synthesis Pd NPs, believing that the *S. Mukorossi* extract would act as a reducing agent as well as an efficient surfactant to stabilize the Pd NPs.

Fig. 1. Image of *Sapindus mukorossi* and dried seeds

The main components of the aqueous extract of *S. Mukorossi* fruit pericarp (soapnut shell) are mainly saponins (natural surfactants), flavonoids and carbohydrates [17]. These constituents are mainly responsible for its reduction potential. They are mainly used for washing purpose by the native people of Asia. Apart from this, they also have some medicinal properties like anti-inflammatory [18] and anti-microbial activity [19]. Reddy and co-workers reported a method for the synthesis of Au NPs using *S. Mukorossi* fruit pericarp (soapnut shell) extract and thereafter they evaluated their catalytic activity for reduction of *p*-nitroaniline [16].

3.2. Experimental

3.2.1. General Information

All the reactions were carried out under open air. ^{1}H and ^{13}C NMR spectra of the synthesized compounds were recorded in a 400 MHz NMR spectrophotometer (JEOL, JNM-ECS) using tetramethylsilane (TMS) as the internal standard. Chemical shifts are expressed in ppm and the coupling constants are expressed in Hertz. The reactions were monitoring by using thin-layer-chromatography (TLC) technique employing aluminium precoated TLC plates with silica gel $60F_{254}$ (Merck). The spots were visualized using UV light and iodine vapour. Purification of the products was done by column chromatography technique using silica gel (60-120 mesh). Melting point was recorded in Büchi B450 melting point apparatus. UV-Visible spectral analysis was done in Shimadzu (UV-2550) UV-Vis spectrophotometer, FT-IR spectra were recorded in a Nicolet (Impact 410) FT-IR spectrophotometer with frequencies expressed in wave numbers (cm^{-1}). The

powder XRD pattern was recorded with Rigaku X-ray diffractometer over the range of 2θ =10-80°. It uses Cu K radiation source (0.15419 nm) and has scintillation counter detector. The EDX analysis of the prepared catalyst was done in JEOL SEM (JEOL, model JSM-6390 LV operating at an accelerating voltage of 15 kV). Size and distribution of NPs were determined by using JEOL TEM (JEM-2010) equipped with a slow-scan CCD camera at an operating voltage of 200kV. Flame photometry test was done in a Flame photometer (Systronics-128).

3.2.2. Materials and chemical reagents

All the Chemicals were purchased from different commercials firms. Palladium acetate and phenylboronic acids were purchased from Alfa-Aesar, potassium carbonate from Qualigens, bromobenzene from G.S. Chemical Testing Labs, Bombay, India and all other chemicals were purchased from Sisco-Research-Laboratories Pvt. Ltd. India. Hexane and ethyl acetate that were used for purification purposes were distilled prior to use. All the other chemicals were used without further purification.

3.2.3. Preparation of the catalyst

Soapnut seed shells were first collected cleaned and shade dried. After proper drying the seeds were grounded by using domestic blender. For the preparation of plant extract, 10 g of the finely ground seeds was added to 60 mL distilled water in a beaker and then stirred at 60 °C for about 30 min. Finally, the whole content was filtered with muslin cloth at ambient temperature. The filtrate was called as aqueous extract and was kept for further experiment.

For preparing the nanocatalyst, 10 mL of the aqueous extract was added to 25 mL of 1 mM $Pd(OAc)_2$ solution. The solution was then refluxed in an oil bath for about 2 h. The gradual change of color of the solution from light brown to dark black indicated the formation of NPs. After that, the NPs were separated by centrifuging at 12,000 rpm for 15 min. The Pd NPs were then washed with distilled water and ethanol, for making them free from biomaterials and finally dried in an oven at 60 °C for 2 h.

3.2.4. General procedure for Suzuki-Miyaura coupling reaction

To investigate the catalyst for Suzuki-Miyaura reaction, phenylboronic acid and *p*-bromonitrobenzene were chosen as model substrates. A mixture of *p*-bromonitrobenzene (0.5 mmol), phenylboronic acid (0.55 mmol), K_2CO_3 (1.5 mmol), nanocatalyst (5 wt% with respect to boronic acid) were added to a 50 mL round-bottomed flask, and stirred at room temperature in *iso*-propanol:water (1:1) solvent system for the required time. No ligand or additive was added during the course of the reaction. The monitoring of the reaction was done by TLC technique. After completion, the reaction mixture was first diluted with distilled water and then distilled ethyl acetate was used to extract the product from the reaction mixture (3 times). Thereafter it was washed with brine (3 times) and then anhydrous Na_2SO_4 was used for removal of traces of water left. Finally, column chromatography technique (60-120 mesh silica gel and ethyl acetate-hexane solvent mixture) was used to purify the product and confirmed by ^1H and ^{13}C NMR spectroscopy.

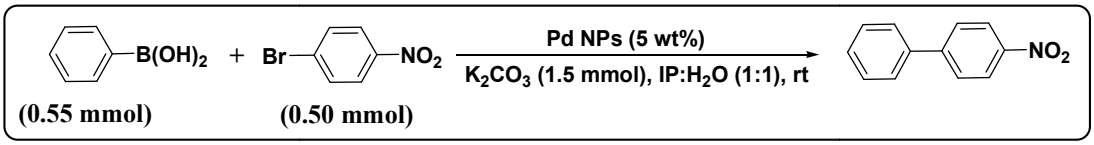

Scheme 1: Model reaction for Suzuki-Miyaura cross-coupling reaction.

3.3. Results and Discussion

3.3.1. Characterization of the Soapnut shell

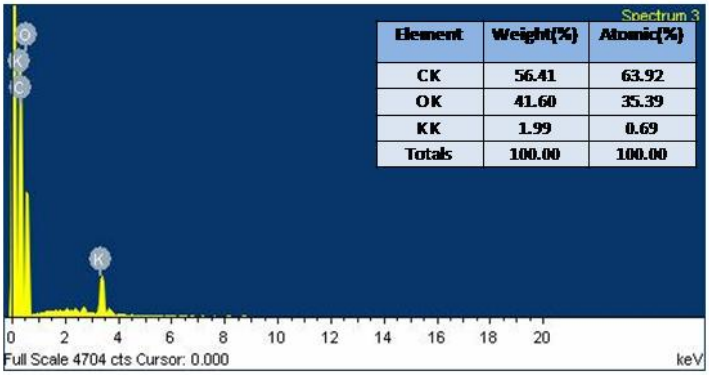

Fig. 2: EDX image of ground *S. mukorossi* Seed.

To know the elemental composition, the soapnut shells powder was first characterized by EDX analysis (Fig. 2). The EDX analysis indicates the presence of element potassium (K) in addition to carbon (C) and oxygen (O). However, compared to C (63.92%) and O (35.39%), the amount of K is very low (0.69%). Further, flame photometry test also confirmed the presence of low amount of K (0.046%).

3.3.2. Characterization of the catalyst, Pd NPs@PEG

3.3.2.1. UV-Visible Spectroscopic analysis

The formation of Pd NPs in presence of *S. mukorossi* seed extract was confirmed by examining the solution after 30 min and after 2 h with the help of UV-Visible spectroscopy. The presence of peak near about 400 nm in the UV-visible spectrum (Fig. 3) corresponds to Pd(II) of the aqueous solution of $Pd(OAc)_2$ dissolved with a few drops of ethanol. However, with the formation of Pd NPs, the peak near 400 nm commenced to disappear and vanished completely in 2 h indicating that Pd(II) was completely reduced to Pd(0) and thus suggesting the formation of Pd NPs.

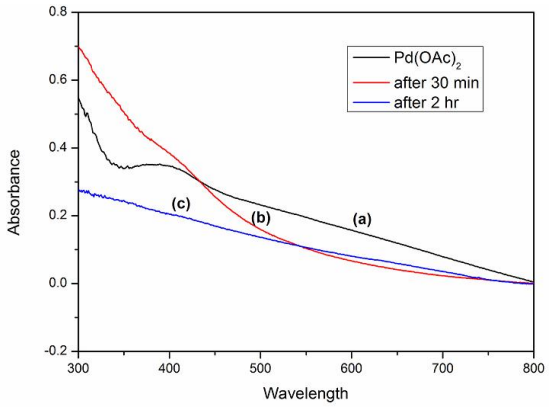

Fig. 3: UV-visible spectra of (a) $Pd(OAc)_2$, (b) after 30 min and (c) after 2 h.

3.3.2.2. Powder XRD and EDX analyses

Powder XRD technique was used to determine the crystalline nature of the synthesized Pd NPs. Three distinct picks at 40.010°, 46.040° and 67.790° were observed in the XRD pattern [Fig 4(a)], which correspond to (111), (200) and (220) planes respectively that could be indexed to fcc phase of Pd NPs (JCPDS ≠88-2335). The widening of the XRD

peak suggests that the synthesized particles are in nano range. Fig. 4(b) shows the EDX analysis of the Pd NPs which indicates the presence of Pd devoid of any other metal impurities.

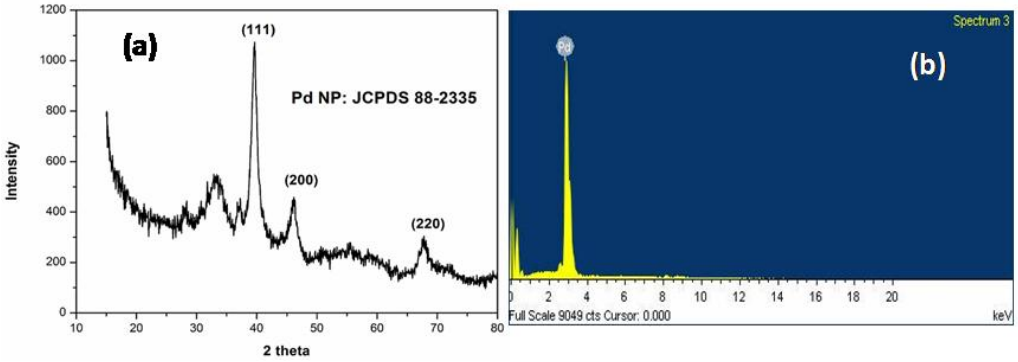

Fig. 4: (a) PXRD pattern and (b) EDX pattern of synthesized Pd NPs.

3.3.2.3. TEM and particle size distribution analyses

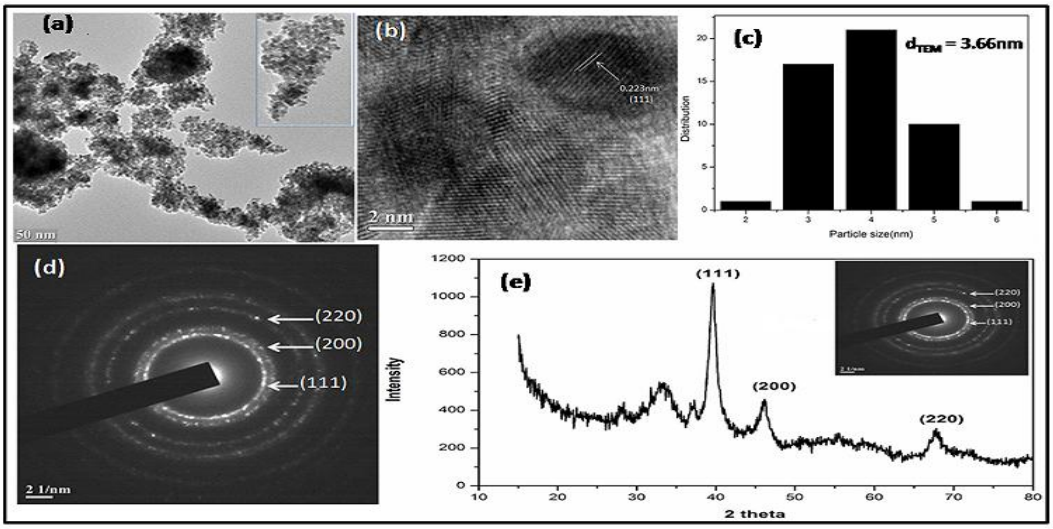

Fig. 5 (a) TEM and (b) HRTEM images of Pd NPs, (c) particle size distribution plot, (d) SAED pattern and (e) comparison between SAED and XRD pattern of Pd NPs.

The synthesized NPs are characterized for size and shape by using TEM and HRTEM as shown in Fig 5. The TEM image suggests that the NPs preferentially crystallize in spherical shape. The inter planer distance calculated from the HRTEM image (0.223 nm) corresponds to (111) plane of Pd NPs [Fig. 5(b)]. It is obvious from the size distribution

plot [Fig. 5(c)] that most of the particles fall in the range 3-5 nm and the average particle diameter is found to be about 3.6 nm. Because of this smaller size of the Pd NPs they have high surface area and thus show high catalytic activity. The SAED image as shown in the Fig. 5(d) clearly shows diffraction dots which proves the crystalline nature of the synthesized Pd NPs and the crystal lattices corresponding to the (111), ((200) and (220) planes are clearly visible. The comparison between the XRD planes and the SAED pattern is shown in Fig. 5(e).

3.3.3. Role of soapnut shells in bioreduction process

The main bioactive component present in the aqueous extract of soapnut shells are saponins and flavonoids. A numbers of hydroxyl groups are present in these biomolecules which actually participate in the reduction of Pd(II) to Pd(0). The bio-reduction of Pd(II) to Pd(0) is believed to occur through the oxidation of hydroxyl groups to carbonyl groups as shown below:

$$Pd(II) + 2R\text{-}OH \longrightarrow Pd(0) + 2R=O + 2H^{+}$$

The peak observed at 3439 cm^{-1} in the IR spectrum of plant extract [Fig. 6(a)] is due to O-H stretching vibration of saponins or flavonoids. The carboxylic O-H bond stretching of saponins or flavonoids gives a low intense peak at 2851 cm^{-1} [16]. The peak position at 1635 cm^{-1} is due to the presence of C=C groups in saponins [20]. Additionally, the indication of a peak at 1016 cm^{-1} specifies the presence of ester groups in saponins

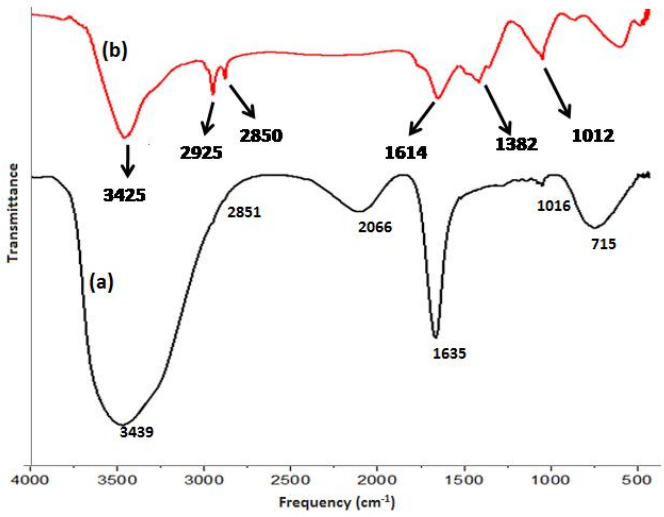

Fig. 6: FT IR spectra of (a) soapnut shell extract and (b) Pd NPs.

[20]. The presence of peak at 2066 cm^{-1} in the FTIR spectrum is due to the C-H stretching vibration of sugar present in the soapnut shells extract [14]. The hydroxyl groups that are present in the aqueous extract of soapnut shells extract are primarily responsible for the reduction of Pd(II) to Pd(0). In the IR spectrum of Pd NPs [Fig. 6(b)], the appearance of peaks at 2850, 1614 and 1012 cm^{-1} shows that the resulting Pd NPs might be stabilized by the functional groups present in the biomolecules of soapnut shells extract.

3.3.4. Optimization of the reaction condition

After characterization of the synthesized Pd NPs, our next aim was to find out a suitable reaction condition for the Suzuki-Miyaura coupling reaction. The substrates chosen for the model reaction were 4-bromonitrobenzene and phenylboronic acid. It is worth to mention that the system shows remarkably good catalytic activity for coupling of phenylboronic acids with inactivated aryl bromides in *iso*-propanol: water (1:1) at room temperature. The results are summarized in table 1.

Initially, the effect of solvent on the reaction was screened using K_2CO_3 (1.5 mmol) as base which showed that *iso*-propanol:H_2O (1:1) was the most effective one, affording excellent yield (entry 6, Table 1). It is clear from entry 2 of table 1 that presence of base is also very essential for the reaction, as the reaction does not proceed in the absence of base. Other inorganic bases like Na_2CO_3, KOH etc. also have positive effect on the reaction and proceeds with comparable yield of the cross-coupling product (entries 7 & 8, Table 1). Again optimizing the reaction condition for the amount of the catalyst, we found that 5 wt% of the nanocatalyst was the optimized amount for best conversion. Again it is obvious from table 1 that as we decreased the amount of base, K_2CO_3 to 1 mmol (entry 12, Table 1) the yield also decreased to 87%.

Thus, from above discussion it was distinct that 5 wt% of the catalyst in *iso*-propanol:water(1:1) solvent and in the presence of K_2CO_3 (1.5 mmol) base at room temperature was the best reaction condition for the formation of biaryl (entry 6, Table 1).

Table 1: Optimization of reaction[a]:

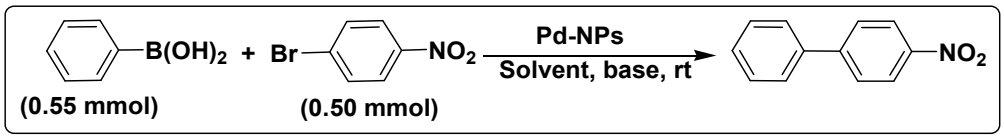

Entry	Amount of catalyst (wt%)	Solvent	Base (1.5 mmol)	Time (h)	Yield[b] (%)
1	5	No solvent	K_2CO_3	8	15
2	5	H_2O	No base	24	….
3	5	H_2O	K_2CO_3	24	60
4	5	DMF	K_2CO_3	24	74
5	5	MeOH:H_2O	K_2CO_3	24	80
6	**5**	**Isopropanol:H_2O**	**K_2CO_3**	**0.5**	**94**
7	5	Isopropanol:H_2O	Na_2CO_3	1.5	90
8	5	Isopropanol:H_2O	KOH	2.5	85
9	3	Isopropanol:H_2O	K_2CO_3	3	82
10	8	Isopropanol:H_2O	K_2CO_3	0.5	94
11	10	Isopropanol:H_2O	K_2CO_3	0.5	94
12[c]	5	Isopropanol:H_2O	K_2CO_3	0.5	87

[a]Reaction condition: Phenylboronic acid (0.55 mmol), 4-bromonitrobenzene (0.50 mmol), rt. [b]Isolated yield. [c]1mmol of base was used.

3.3.5. Substrate study

With the optimized reaction condition having defined, we next evaluated the scope and limitation of the above reaction procedure, with wide varieties of electronically diverse arylhalides with arylboronic acids. The results are summarized in Table 2.

From the substrate study, it is clear that cross-coupling reaction between aryl halides and arylboronic acids bearing different electron-withdrawing and electron-donating groups proceeds smoothly by the synthesized Pd NPs. However, if the aryl boronic acid contains electron donating groups (entries 6-8, Table 2), the reaction proceeded smoothly requiring less reaction time as compared to aryl boronic acid containing electron withdrawing groups (entries 10-12, Table 2).

Table 2: Suzuki-Miyaura cross-coupling reactions of various aryl halides and arylboronic acids catalyzed by Pd NPs:[a]

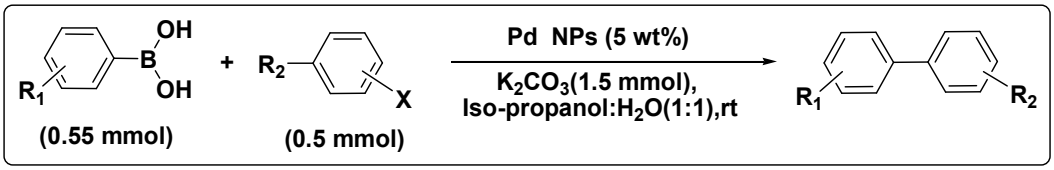

Entry	R_1	R_2	X	Time (min)	Yield[b] (%)
1	H	H	Br	30	95
2	H	H	I	20	96
3	H	NO_2	4-Br	30	94
4	H	OCH_3	4-I	15	85
5	4-Cl	NO_2	4-Br	45	95
6	4-OCH_3	H	4-Br	50	81
7	4-OCH_3	OCH_3	4-I	25	98
8	4-CH_3	OCH_3	4-Br	40	89
9	4-CHO	H	4-Br	40	89
10	4-CHO	OCH_3	4-Br	80	85
11	4-$COCH_3$	H	4-Br	80	85
12	4-$COCH_3$	OCH_3	4-I	65	85
13	4-F	OCH_3	4-Br	80	89

[a]Reaction Conditions: arylbromide or iodide (0.5 mmol), arylboronic acid (0.55 mmol), Pd NPs (5 wt%), K_2CO_3 (1.5 mmol), rt, in air. [b]Isolated yield.

3.3.6. Reusability study

Again, according to the perspective of green chemistry, the reusability of the catalysts is an important parameter. Accordingly, we examine the reusability of our catalyst by using the model substrates, phenylboronic acid (1.1 mmol) and 4-bromonitrobenzene (1 mmol) (Scheme 1). For recovery purpose, the scale of the model reaction was increased to two folds. From Fig. 7 it is obvious that the catalyst was reusable up-to 5th cycle with slight loss of catalytic activity. After 5th cycle, the catalytic activity decreased sharply which might be due to deactivation of the catalyst during the course of reaction and recovery process as shown in Fig. 7. Here, in order to fix the stability issue of the Pd NPs, we employed TEM imaging technique before and after the Suzuki reaction. Figs. 8(a) and

8(b) represent the TEM image and the corresponding particle size distribution of the Pd NPs before the reaction. [Figs. 8(a) and 8(b) are same with Figs. 5(a) and 5(c) respectively]. The TEM image of Pd NPs after 2nd cycle and their corresponding particle size distribution are presented in Figs. 8(c) and 8(d) respectively. Now it is clear that there was no change of NPs size before and after the second cycle. [Comparing Fig. 8(b) with 8(d)]. The TEM image of the particles after 5th cycle and their corresponding particle size distributions are shown in Figs. 8(e) and 8(f) respectively. The average size of the NPs was calculated from Fig. 8(f) and was found to be 4.74 nm. Generally, the catalytic activity of the nanocatalyst is determined by the size of the NPs. Smaller the size, the more is its catalytic activity. As after 5th cycle the size of the NPs increases, its catalytic activity also decreases. It may be due to the fact that the stabilizing effect of the biomolecules present in the soapnut shells extract over the surface of Pd NPs deteriorated after 5th cycle and therefore aggregation of Pd NPs took place and consequently the size of the NPs became larger. Because of this the catalytic activity of the Pd NPs decreased after 5th cycle.

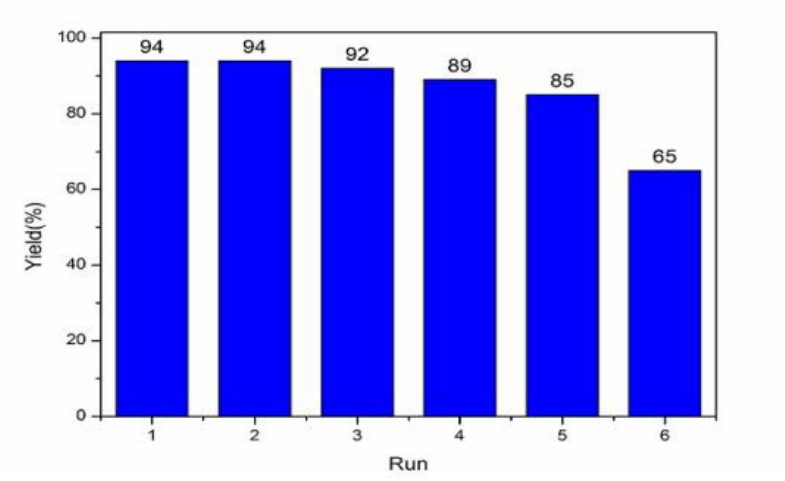

Fig. 7: Reusability of Pd nanocatalyst.

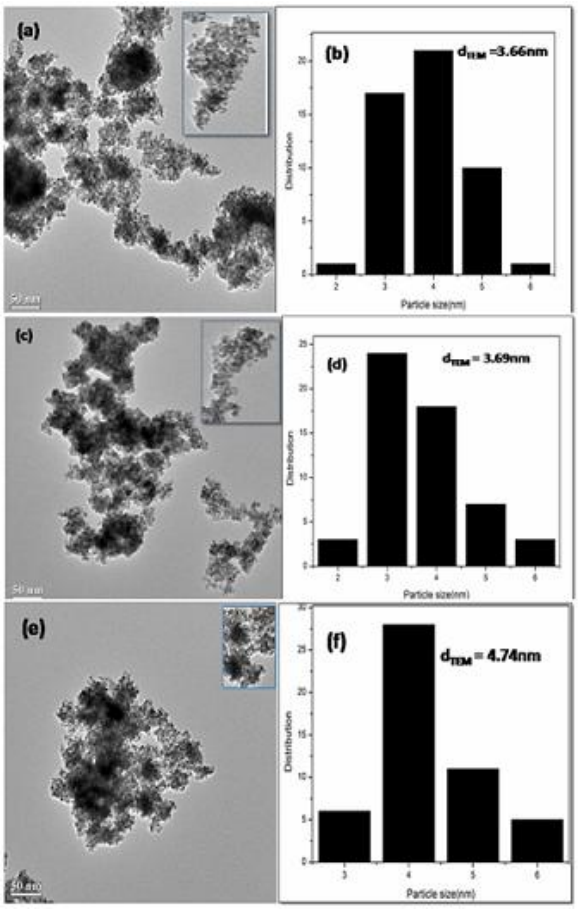

Fig 8. TEM images of Pd NPs (a) before the reaction, (c) after second cycle, (e) after fifth cycle, and (b), (d) and (f) are their corresponding particle size distribution.

3.3.7. Hot filtration study

To check the heterogeneous nature of the catalyst hot filtration test is a technique was done (Fig. 9). To do this the model reaction was again performed under optimized reaction conditions. After 15 min, the reaction was stopped and the catalyst was filtered off from the reaction. The reaction was found to be approximately 51% complete at this point. After removal of the catalyst through filtration, the reaction was monitored under the same reaction condition for an additional 10 h. However, we didn't observe any significant increase in the yield of the cross-coupled product, which proves the heterogeneity of the catalyst.

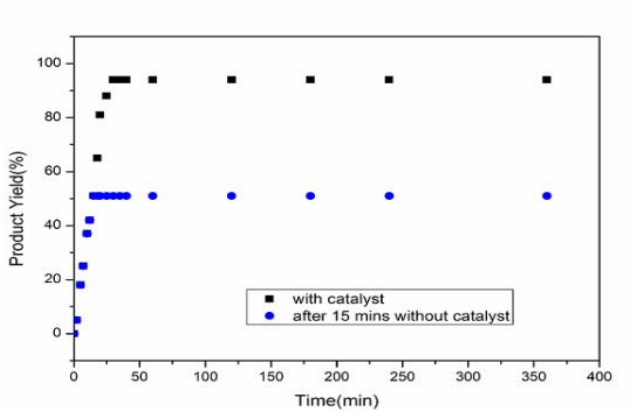

Fig. 9: Hot filtration test of the catalyst.

3.4. Conclusions

In conclusion, an efficient and green protocol for the synthesis of Pd NPs using *S. mukorossi* seed extract has been developed which exhibits excellent catalytic activity under ligand free conditions for Suzuki-Miyaura cross-coupling reaction at room temperature. The saponin and flavonoid compounds present in the soapnut shells are mainly responsible for the reduction of Pd(II) which eliminates the use of toxic reducing agents. Therefore, we can consider the process for the synthesis of Pd NPs as green synthesis and might be useful for the synthesis of other transition metal NPs.

Characterization data of the products

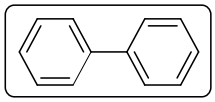

Biphenyl (entries 1 & 2, Table 2): White crystal, m.p. 69.2 °C, ^{1}H NMR (400 MHz, $CDCl_3$) δ (ppm): 7.64 (m, 4H), 7.48 (m, 4H), 7.40 (m, 2H); ^{13}C NMR (100 MHz, $CDCl_3$) δ (ppm): 141.3, 128.8, 127.3, 127.2.

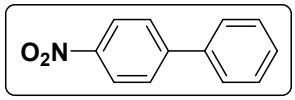

4-Nitrobiphenyl (entry 3, Table 2): Yellow solid, m.p. 113 °C,^{1}H NMR (400 MHz, $CDCl_3$) δ (ppm): 8.31 (m, 2H), 7.75-7.73 (m, 2H), 7.62-7.61 (m, 2H), 7.52-7.45 (m, 3H); ^{13}C NMR (100 MHz, $CDCl_3$) δ (ppm): 147.7, 147.1, 138.8, 129.2, 129.0, 127.8, 127.4, 124.1.

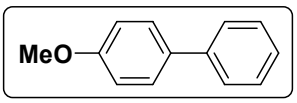

4-Methoxybiphenyl (entries 4 & 6, Table 2): White crystal, m.p. 90 °C, ^{1}H NMR (400 MHz, $CDCl_3$) δ (ppm): 7.55 (m, 4H), 7.41 (t, *J*=4Hz, 2H), 7.29 (t, *J*=8Hz, 1H), 6.97 (d, *J*=8Hz, 2H), 3.84 (s, 3H); ^{13}C NMR (100 MHz, $CDCl_3$) δ (ppm): 159.2, 140.9, 133.8, 128.8, 128.2, 126.8, 126.7, 114.2, 55.4.

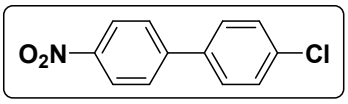

4-Chloro-4′-nitrobiphenyl (entry 5, Table 2):White crystal, m.p. 141 °C, ^{1}H NMR (400 MHz, $CDCl_3$), δ (ppm): 8.30 (d, *J*=8Hz, 2H), 7.70 (d, *J*=8Hz, 2H), 7.56 (d, *J*=8Hz, 2H), 7.47 (d, *J*=8Hz, 2H); ^{13}C NMR (100 MHz, $CDCl_3$), δ (ppm): 147.3, 146.4, 137.2, 135.3, 129.4, 128.7, 127.7, 124.3.

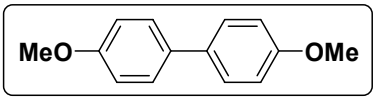

4,4′-dimethoxybiphenyl (entry 7, Table 2): White Crystalline solid, m.p. 175.5 °C, ^{1}H NMR (400 MHz, $CDCl_3$) δ (ppm): 7.47 (d, *J*=8Hz, 4H), 6.95 (d, *J*=8Hz, 4H), 3.84 (s, 6H); ^{13}C NMR (100 MHz, $CDCl_3$) δ (ppm): 158.7, 133.5, 127.8, 114.2, 55.4.

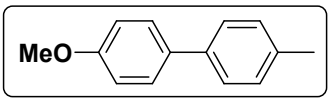

4-Methyl-4′-methoxybiphenyl (entry 8, Table 2): White crystal, m.p. 105 °C, ^{1}H NMR (400 MHz, $CDCl_3$) δ (ppm): 7.51 (d, *J*=8Hz, 2H), 7.44 (d, *J*=8Hz, 2H), 7.22 (d, *J*=8Hz, 2H), 6.96 (d, *J*=8Hz, 2H), 3.84 (s, 3H); ^{13}C NMR (100 MHz, $CDCl_3$) δ (ppm): 158.9, 138.0, 136.4, 133.8, 129.5, 128.0, 126.6, 114.2, 55.4, 21.1.

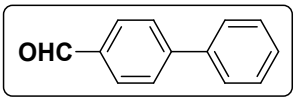

4-Formylbiphenyl (entry 9, Table 2): Light yellow crystal, m.p. 58 °C, ^{1}H NMR (400 MHz, $CDCl_3$) δ (ppm): 10.05 (s, 1H), 7.96-7.94 (m, 2H), 7.75 (d, *J*=8Hz, 2H), 7.65-7.62

(m, 2H), 7.50-7.46 (m, 2H), 7.42 (d, *J*=8Hz, 1H); ^{13}C NMR (100 MHz, $CDCl_3$) δ (ppm): 192.0, 147.3, 139.7, 135.2, 130.3, 129.1, 128.5, 127.7, 127.4.

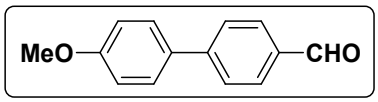

4-Formyl-4′-methoxybiphenyl (entry 10, Table 2): White crystal, m.p. 98 °C, ^{1}H NMR (400 MHz, $CDCl_3$) δ (ppm): 10.03 (s, 1H), 7.92 (d, *J*=8Hz, 2H), 7.71 (d, *J*=8Hz, 2H), 7.59 (d, *J*=8Hz, 2H), 7.01 (d, *J*=8Hz, 2H), 3.87 (s, 3H); ^{13}C NMR (100 MHz, $CDCl_3$) δ (ppm): 191.9, 160.2, 146.5, 134.7, 132.1, 130.4, 128.5, 127.1, 114.5, 55.4.

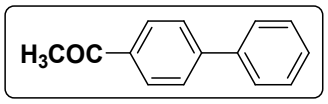

4-Acetylbiphenyl (entry 11, Table 2): White crystal, m.p. 118 °C, ^{1}H NMR (400 MHz, $CDCl_3$) δ (ppm): 8.0 (d, *J*=12Hz, 2H), 7.69 (d, *J*=8Hz, 2H), 7.63 (d, *J*=8Hz, 2H), 7.49-7.46 (t, *J*=8Hz, 2H), 7.41 (d, *J*=8Hz, 1H), 2.64 (s, 3H); ^{13}C NMR (100 MHz, $CDCl_3$) δ (ppm): 190.5, 157.0, 139.9, 135.9, 129.0, 128.3, 127.3, 26.7.

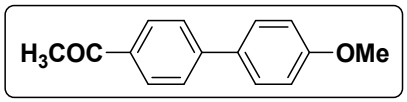

4-Acetyl-4′-methoxybiphenyl (entry 12, Table 2): White crystal, m.p. 153 °C, ^{1}H NMR (400 MHz, $CDCl_3$) δ (ppm): 8.01 (d, *J*=8Hz, 2H), 7.64 (d, *J*=8Hz, 2H), 7.58 (d, *J*=8Hz, 2H), 7.00 (d, *J*=8Hz, 2H), 3.86 (s, 3H), 2.63 (s, 3H); ^{13}C NMR (100 MHz, $CDCl_3$) δ (ppm): 187.4, 145.3, 132.3, 129.0, 128.4, 126.7, 114.4, 98.4, 87.2, 55.4, 26.7.

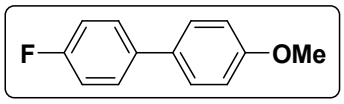

4-Fluro-4′-methoxybiphenyl (entry 13, Table 2): White crystal, m.p. 110 °C, ^{1}H NMR (400 MHz, $CDCl_3$) δ (ppm): 7.48-7.45 (m, 4H), 7.09 (m, 2H), 6.98-6.95 (m, 2H), 3.85 (s, 3H); ^{13}C NMR (100 MHz, $CDCl_3$) δ (ppm): 163.3, 159.1, 137.0, 132.9, 128.3, 128.1, 115.7, 115.5, 114.3, 55.4.

^{1}H NMR spectrum of 4-formylbiphenyl:

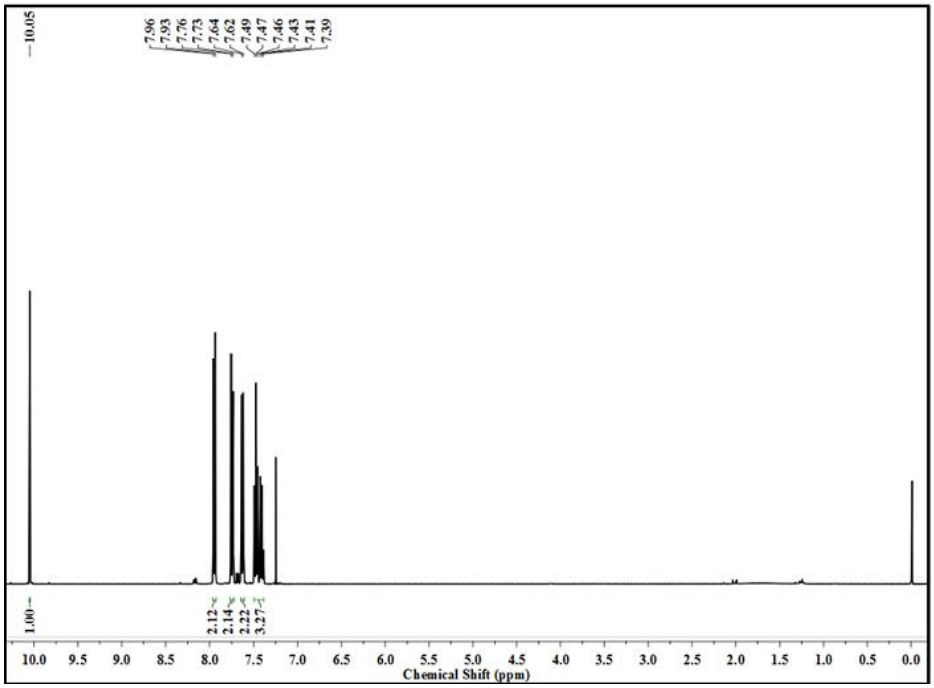

13C NMR spectrum of 4-formylbiphenyl:

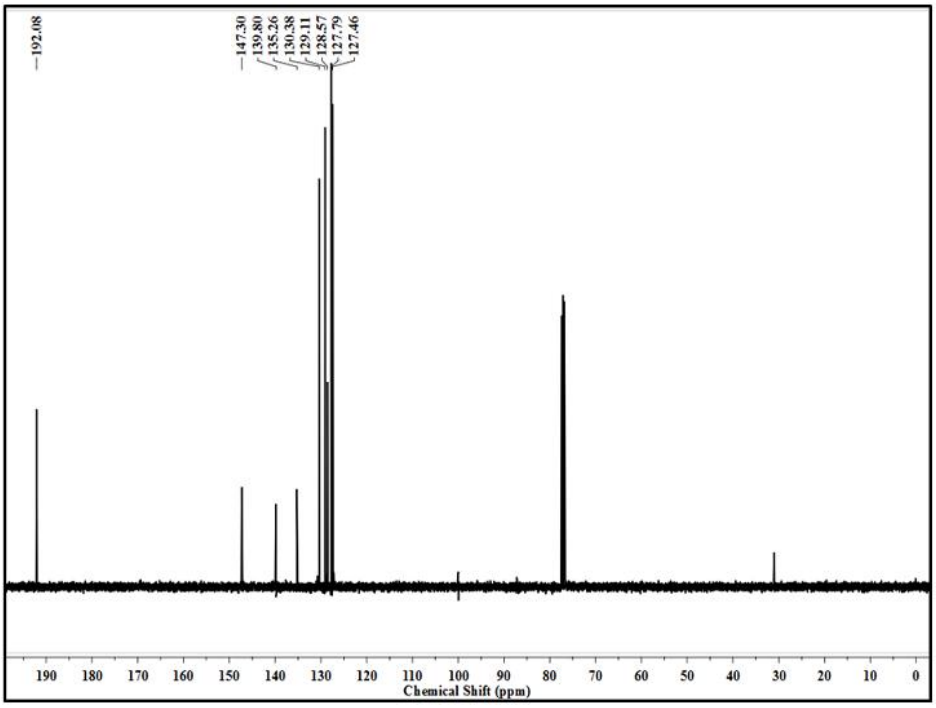

References

[1] Torborg, C. and Beller, M. Recent applications of palladium-catalyzed coupling reactions in the pharmaceutical, agrochemical, and fine chemical industries. *Advanced Synthesis & Catalysis*, 351(18):3027-3043, 2009.

[2] Magano, J. and Dunetz, J. R. Large-scale applications of transition metal-catalyzed couplings for the synthesis of pharmaceuticals. *Chemical Reviews*, 111(3):2177-2250, 2011.

[3] Miyaura, N., Yanagi, T., and Suzuki, A. The palladium-catalyzed cross-coupling reaction of phenylboronic acid with haloarenes in the presence of bases. *Synthetic Communications*, 11(7):513-519, 1981.

[4] (a) Fleckenstein, C. A. and Plenio, H. Sterically demanding trialkylphosphines for palladium-catalyzed cross coupling reactions—alternatives to $PtBu_3$. *Chemical Society Reviews*, 39(2):694-711, 2010. (b) Navarro, O., Kaur, H., Mahjoor, P., and Nolan, S. P. Cross-coupling and dehalogenation reactions catalyzed by (N-heterocyclic carbene)Pd(allyl)Cl complexes. *The Journal of Organic Chemistry*, 69(9):3173-3180, 2004. (c) da Costa, D. P. and Nobre, S. M. Bisamides as ligands in Suzuki coupling reactions catalyzed by palladium. *Tetrahedron Letters*, 54(34):4582-4584, 2013. (d) Banik, B., Tairai, A., Shahnaz, N., and Das, P. Palladium (II) complex with a potential N4-type Schiff-base ligand as highly efficient catalyst for Suzuki–Miyaura reactions in aqueous media. *Tetrahedron Letters*, 53(42):5627-5630, 2012. (e) Dewan, A., Buragohain, Z., Mondal, M., Sarmah, G., Borah, G., and Bora, U. Acetanilide palladacycle: an efficient catalyst for room-temperature Suzuki–Miyaura cross-coupling reaction. *Applied Organometallic Chemistry*, 28(4):230-233, 2014.

[5] (a) Lindström, U. M. Stereoselective organic reactions in water. *Chemical Reviews*, 102(8):2751-2772, 2002. (b) Herrerias, C. I., Yao, X., Li, Z., and Li, C. J Reactions of C− H bonds in water. *Chemical Reviews*, 107(6):2546-2562, 2007.

[6] Sheldon, R. Catalytic reactions in ionic liquids. *Chemical Communications*, 23:2399-2407, 2001.

[7] Mayadevi, S. Reactions in supercritical carbon dioxide. *Indian J. Chem*. 51A:1298, 2012.

[8] (a) Pérez-Lorenzo, M. Palladium nanoparticles as efficient catalysts for Suzuki cross-coupling reactions. *The Journal of Physical Chemistry Letters*, 3(2):167-174, 2012. (b) Das, S. K., Parandhaman, T., Pentela, N., Islam, M., A. K. M., Mandal, A. B., and Mukherjee, M. Understanding the biosynthesis and catalytic activity of Pd, Pt, and Ag nanoparticles in hydrogenation and Suzuki coupling reactions at the nano–bio interface. *The Journal of Physical Chemistry C*, 118(42):24623-24632, 2014.

[9] (a) Huang, Y. B., Wang, Q., Liang, J., Wang, X., and Cao, R. Soluble metal-nanoparticle-decorated porous coordination polymers for the homogenization of heterogeneous catalysis. *Journal of the American Chemical Society*, 138(32):10104-10107, 2016. (b) Huang, Y., Zheng, Z., Liu, T., Lü, J., Lin, Z., Li, H., and Cao, R. Palladium nanoparticles supported on amino functionalized metal-organic frameworks as highly active catalysts for the Suzuki–Miyaura cross-coupling reaction. *Catalysis Communications*, 14(1):27-31, 2011.

[10] (a) Rao, C. R., Kulkarni, G. U., Thomas, P. J., and Edwards, P. P. Metal nanoparticles and their assemblies. *Chemical Society Reviews*, 29(1):27-35, 2000. (b) Planellas, M., Pleixats, R. and Shafir, A. Palladium nanoparticles in Suzuki cross-couplings: Tapping into the potential of Tris-Imidazolium salts for nanoparticle stabilization. *Advanced Synthesis & Catalysis*, 354(4):651-662, 2012.

[11] (a) Nasrollahzadeh, M., Atarod, M., Jaleh, B., and Gandomirouzbahani, M. *In situ* green synthesis of Ag nanoparticles on graphene oxide/TiO_2 nanocomposite and their catalytic activity for the reduction of 4-nitrophenol, congo red and methylene blue. *Ceramics International*, 42(7):8587-8596, 2016. (b) Nasrollahzadeh, M., Sajadi, S. M., Rostami-Vartooni, A., Alizadeh, M., and Bagherzadeh, M. Green synthesis of the Pd nanoparticles supported on reduced graphene oxide using barberry fruit extract and its application as a recyclable and heterogeneous catalyst for the reduction of nitroarenes. *Journal of Colloid and Interface Science*, 466:360-368, 2016. (c) Atarod, M., Nasrollahzadeh, M., and Sajadi, S. M. Green synthesis of Pd/RGO/Fe_3O_4 nanocomposite using Withania coagulans leaf extract and its application as magnetically separable and reusable catalyst for the reduction of 4-nitrophenol. *Journal of Colloid and Interface Sscience*, 465:249-258, 2016. (d) Nasrollahzadeh, M., Sajadi, S. M., and Hatamifard, A. Waste chicken eggshell as a natural valuable resource and environmentally benign support for biosynthesis of catalytically active Cu/eggshell, Fe_3O_4/eggshell and

Cu/Fe_3O_4/eggshell nanocomposites. *Applied Catalysis B: Environmental*, 191:209-227, 2016. (e) Nasrollahzadeh, M. and Sajadi, S. M. Preparation of Au nanoparticles by Anthemis xylopoda flowers aqueous extract and their application for alkyne/aldehyde/amine A 3-type coupling reactions. *RSC Advances*, 5(57):46240-46246, 2015. (f) Nasrollahzadeh, M., Sajadi, S. M. and Maham, M. Green synthesis of palladium nanoparticles using Hippophae rhamnoides Linn leaf extract and their catalytic activity for the Suzuki–Miyaura coupling in water. *Journal of Molecular Catalysis A: Chemical*, 396:297-303, 2015. (g) Nasrollahzadeh, M., Atarod, M., and Sajadi, S. M. Biosynthesis, characterization and catalytic activity of Cu/RGO/Fe_3O_4 for direct cyanation of aldehydes with $K_4[Fe(CN)_6]$. *Journal of Colloid and Interface Science*, *486*:153-162, 2017.

[12] (a) Nasrollahzadeh, M. Green synthesis and catalytic properties of palladium nanoparticles for the direct reductive amination of aldehydes and hydrogenation of unsaturated ketones. *New Journal of Chemistry*, 38(11):5544-5550, 2014. (b) Nasrollahzadeh, M., Maham, M., and Sajadi, S. M. Green synthesis of CuO nanoparticles by aqueous extract of Gundelia tournefortii and evaluation of their catalytic activity for the synthesis of N-monosubstitutedureas and reduction of 4-nitrophenol. *Journal of Colloid and Interface Science*, 455:245-253, 2015. (c) Rostami-Vartooni, A., Nasrollahzadeh, M., and Alizadeh, M. Green synthesis of perlite supported silver nanoparticles using Hamamelis virginiana leaf extract and investigation of its catalytic activity for the reduction of 4-nitrophenol and Congo red. *Journal of Alloys and Compounds*, 680:309-314, 2016. (d) Nasrollahzadeh, M., Sajadi, S. M., Honarmand, E., and Maham, M. Preparation of palladium nanoparticles using Euphorbia thymifolia L. leaf extract and evaluation of catalytic activity in the ligand-free Stille and Hiyama cross-coupling reactions in water. *New Journal of Chemistry*, 39(6):4745-4752, 2015. (e) Nasrollahzadeh, M., Sajadi, S. M., Rostami-Vartooni, A., and Khalaj, M. Green synthesis of Pd/Fe_3O_4 nanoparticles using Euphorbia condylocarpa M. bieb root extract and their catalytic applications as magnetically recoverable and stable recyclable catalysts for the phosphine-free Sonogashira and Suzuki coupling reactions. *Journal of Molecular Catalysis A:Chemical*, 396:31-39, 2015.

[13] Cookson, J. The preparation of palladium nanoparticles. *Platinum Metals Review*, 56(2):83-98, 2012.

[14] Borah, R. K., Saikia, H. J., Das, V. K., and Thakur, A. J. Biosynthesis of poly(ethyleneglycol)-supported palladium nanoparticles using Colocasia esculenta leaf extract and their catalytic activity for Suzuki–Miyaura cross-coupling reactions. *RSC Advances*, 5(89):72453-72457, 2015.

[15] Balakrishnan, S., Varughese, S., and Deshpande, A. P. Micellar characterisation of saponin from Sapindus mukorossi. *Tenside Surfactants Detergents*, 43(5):262-268, 2006.

[16] Reddy, V., Torati, R. S., Oh, S., and Kim, C. Biosynthesis of gold nanoparticles assisted by Sapindus mukorossi Gaertn. Fruit pericarp and their catalytic application for the reduction of p-nitroaniline. *Industrial & Engineering Chemistry Research*, 52(2):556-564, 2012.

[17] Upadhyay, A. and Singh, D. K. Pharmacological effects of Sapindus mukorossi. *Revista do Instituto de Medicina Tropical de São Paulo*, 54(5):273-280, 2012.

[18] Takagi, K., Park, E., and Kato, H. Anti-inflammatory activities of hederagenin and crude saponin isolated from Sapindus mukorossi Gaertn. *Chemical and Pharmaceutical Bulletin*, 28(4):1183-1188, 1980.

[19] Aneja, K. R., Joshi, R., and Sharma, C. In vitro antimicrobial activity of Sapindus mukorossi and Emblica officinalis against dental caries pathogens. *Ethnobotanical leaflets*, 2010(4):3, 2010.

[20] Sharma, V. and Paliwal, R. Isolation and characterization of saponins from Moringa oleifera (moringaceae) pods. *International Journal of Pharmaceutical Sciences*, 5(1):179-183, 2013.